

## Chapter 8

### Dynamic stability analysis – II – Longitudinal motion - 4

#### Lecture 31

#### Topics

#### 8.12 Influence of stability derivatives on SPO and LPO

#### 8.13 Stability diagrams

8.13.1 One parameter stability diagram

8.13.2 Root locus plot

8.13.3 Two parameter stability diagram

#### 8.12 Influence of stability derivatives on SPO and LPO

The discussion in the last two sections leads to the conclusions presented in Table 8.1.

Stability derivative	Item affected	Influence
$X_u$ or $C_D$	Damping of LPO	Increase of $X_u$ increases damping
$Z_u$ or $C_L$	Frequency of LPO	Increase of $Z_u$ increases the frequency
$M_\alpha$ or $C_{m\alpha}$	Frequency of SPO	Increase of $M_\alpha$ increases the frequency
$M_q + M_{\dot{\alpha}}$	Damping of SPO	Increase of $(M_q + M_{\dot{\alpha}})$ increases damping

Table 8.1 Influence of stability derivatives on SPO and LPO

#### Remark:

The term 'E' in the characteristics equation (Eq.8.9) depends on  $C_{m\alpha}$ . When  $C_{m\alpha}$  is zero, 'E' becomes zero (i.e. the airplane has neutral static stability). This reduces the characteristic equation as :

$$A\lambda^4 + B\lambda^3 + C\lambda^2 + D\lambda = 0. \quad (8.63a)$$

This equation has  $\lambda = 0$  as a root.

This indicates neutral dynamic stability(Fig.6.1c). Thus, when the aircraft has neutral static stability, it also has neutral dynamic stability as it should be.

### 8.13 Stability diagrams

From the expressions for the stability derivatives it is observed that they depend on the following.

- a) Flight conditions (h, V or M)
- b) Weight of the airplane (W) and
- c) c.g. location.

Hence, the roots of characteristic equation depend on the choice of these parameters. A diagram, which shows the variation of dynamic stability or the roots of the characteristic equation, with some chosen parameter, is called a stability diagram. Such diagrams are classified into the following types.

(a) One parameter stability diagram, (b) Root locus plot and (c) Two parameter stability diagram.

#### 8.13.1 One parameter stability diagram

In this case a parameter of interest is chosen and the roots of the characteristic equation are obtained for various values of the parameter. Figure 8.6a shows an example of one parameter stability diagram. In the chosen flight condition, the lift coefficient ( $C_L$ ) is equal to one. The parameter chosen to plot the diagram is denoted by ' $\xi$ ' and defined as:

$$\xi = \frac{\bar{m}c}{2\rho S k_B^2} C_L (x_{NP} - x_{cg}) \quad (8.64)$$

Where,  $k_B = \text{radius of gyration} = (I_{yy} / m)^{1/2}$

It may be noted that  $\xi$  is proportional to static margin i.e. ( $- C_{m\alpha}$ ). Consequently, high value of  $\xi$  indicates higher static stability. When  $\xi$  is zero the airplane has neutral static stability. In the present case  $\xi$  or  $C_{m\alpha}$  is varied and the roots of the characteristic equation are calculated. Since,  $\xi$  is plotted on the

Flight dynamics –II  
Stability and control

x-axis in Fig.8.6a, the following special method is adopted to plot the roots. The imaginary part of the complex roots viz. ' $\omega$ ' in the root ( $\eta \pm i \omega$ ) is plotted in the upper part of y-axis. The real parts of the roots are also plotted on the y-axis, the scales on the upper and lower parts of the y-axis may not be the same.

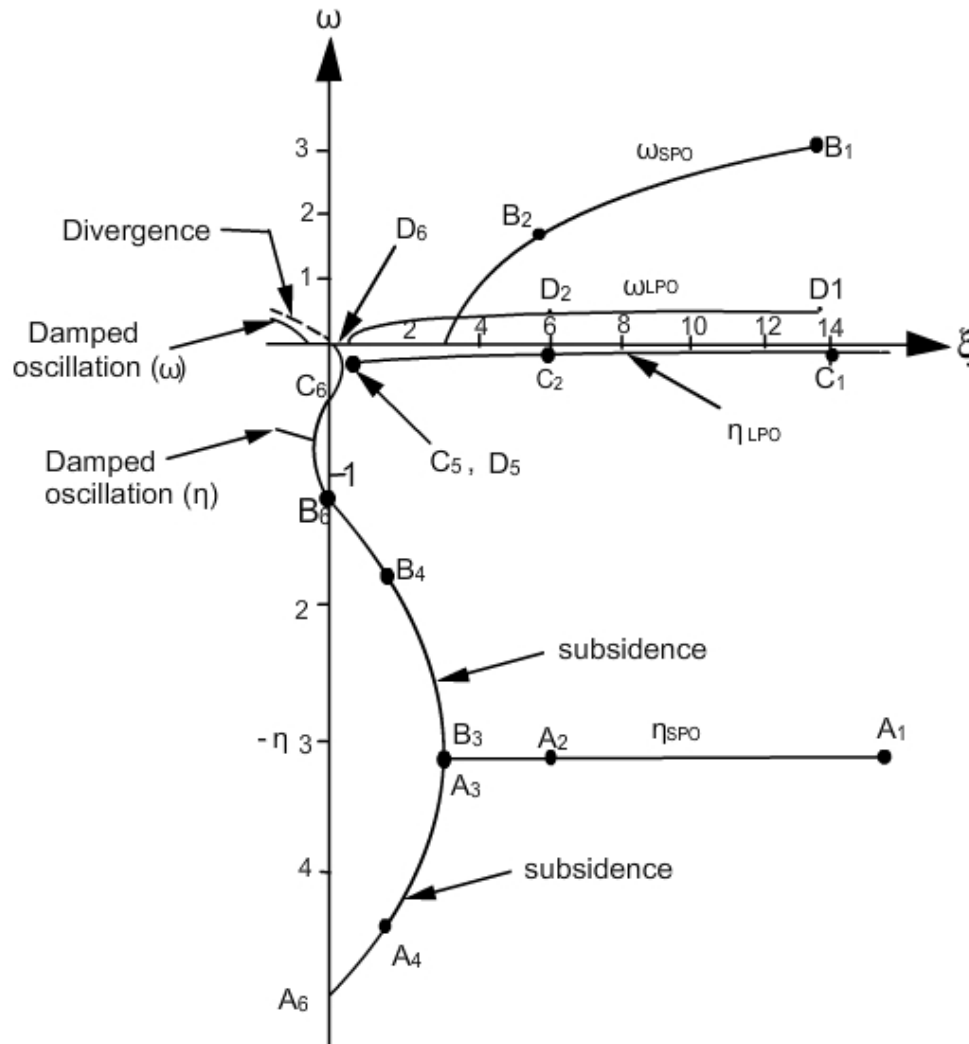


Fig. 8.6a One parameter stability diagram –  $C_L=1$  (Adapted from Ref.1.5, chapter 9 and inturn from Ref.8.1, with permission from controller of HM stationary office)

A brief discussion regarding the points in Fig.8.6a follows.

It may be pointed out Fig.8.6a corresponds to an airplane considered in Ref.8.1.

a) When  $\xi$  is large, say 14, then the roots consist of two complex pairs namely  $-3.2 \pm i 3.2$  and  $-0.06 \pm i 0.47$ . It may be noted that the first pair represents SPO

## Flight dynamics –II

### Stability and control

and the second pair LPO. In the convention for plotting adopted here, the points  $A_1$  and  $B_1$  in Fig.8.6a represent the  $\eta_{SPO}$  and  $\omega_{SPO}$  respectively. The points  $C_1$  and  $D_1$  represent  $\eta_{LPO}$  and  $\omega_{LPO}$  of the second pair (LPO) respectively.

b) As  $\xi$  decreases to a value of nearly six, the roots are represented by points  $A_2, B_2, C_2$  and  $D_2$ . It is observed that the damping of the SPO does not change due to decrease in  $\xi$ . However, the period of SPO increases ( $\omega_{SPO}$  decreases). The damping and the period of the LPO increase slightly with change in  $\xi$ .

c) At  $\xi$  around 3.2 the SPO breaks into two subsidences i.e. instead of a complex pair ( $\eta_{SPO} \pm i \omega_{SPO}$ ), there are two equal real roots  $\lambda_1$  and  $\lambda_2$  with  $\omega_{SPO} = 0$  (see Points  $A_3$  and  $B_3$ ). The damping and period of LPO change marginally. Points  $C_3$  and  $D_3$  are not marked to avoid cluttering of the figure.

d) At  $\xi$  around 1 there are two real roots ( $\lambda_1$  and  $\lambda_2$ ) and a complex pair. The real roots are indicated by points  $A_4$  and  $B_4$ . Points  $C_4$  and  $D_4$  are not marked to avoid cluttering.

e) At  $\xi \approx 0.3$  the LPO also breaks into two subsidences ( $\lambda_3$  and  $\lambda_4$ ) as seen by points  $C_5$  and  $D_5$ . Points  $A_5$  and  $B_5$  are not marked.

f) As  $\xi$  decreases further, four real negative roots are seen. When  $\xi = 0$ , the roots are represented by  $A_6, B_6, C_6$  and  $D_6$ . Note that  $D_6$  equals zero, represents neutral dynamic stability. This is due to the fact that when  $\xi = 0$ , implies that  $C_{m\alpha}$  is also zero. This indicates neutral static stability.

g) For  $\xi < 0$ , one positive root is seen (see the dotted line). When  $\xi$  is less than about 0.4 a positive root, a complex pair and a large negative root are observed.

#### Remarks:

i) Generally low speed airplanes have enough static margin and the roots consist of two complex pairs. But this feature changes when the static margin is low. Fighter airplanes with negative static margin (relaxed static stability) are unstable and need special controls for satisfactory flying.

ii) Figure 8.6b shows one parameter stability diagram at  $C_L = 0.25$ . As mentioned in section 8.12 and Table 8.1, the SPO is not much affected by  $C_L$ , but the period of phugoid (LPO) increases as  $C_L$  decreases.

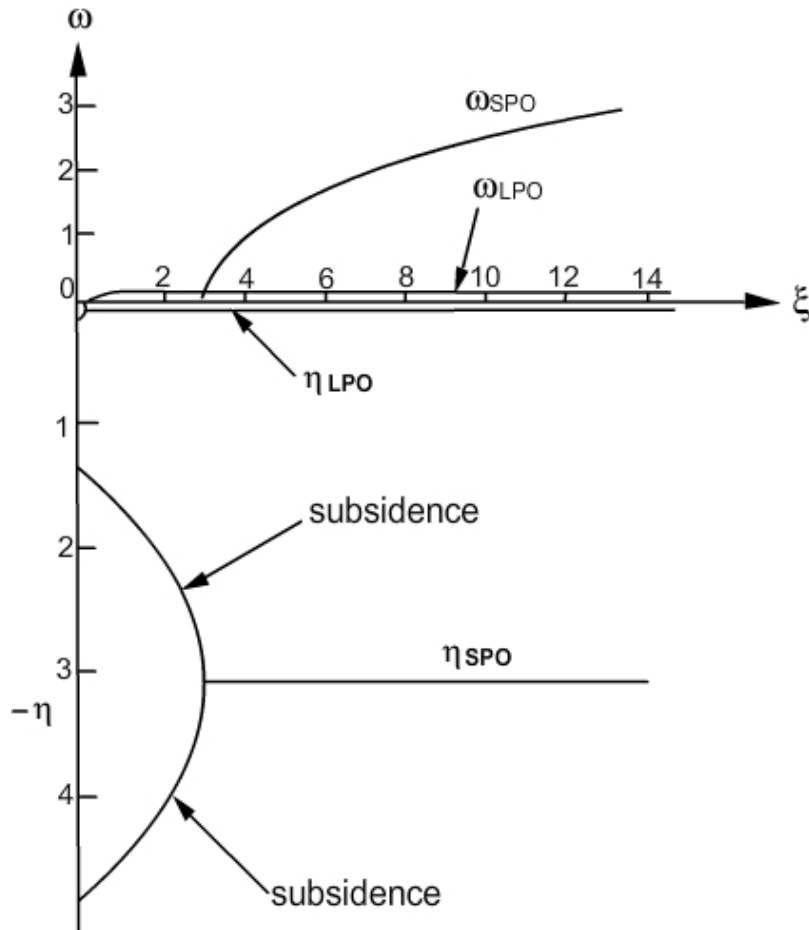


Fig. 8.6b One parameter stability diagram –  $C_L=0.25$

(Adapted from Ref.1.5, chapter 9 and inturn from Ref.8.1, with permission from controller of HM stationary office)

### 8.13.2 Root locus plot

This is another way of plotting the variation of the roots with chosen parameters. Let the complex root be  $r \pm i s$ . A root locus plot is obtained when 'r' is plotted on the x-axis and 's' on the y-axis. A root locus plot corresponding to the information presented in Fig.8.6 a, is plotted in Fig.8.7. Following observations are made.

a) When  $\xi = 14$ , the roots are  $\lambda_{1,2} = -3.2 \pm i 3.2$  and  $\lambda_{3,4} = -0.06 \pm i 0.47$ . Points  $A_1$  and  $B_1$  in Fig.8.7 represent the roots  $\lambda_1$  and  $\lambda_2$  of SPO i.e.  $-3.2 + i 3.2$ , and

Flight dynamics –II  
Stability and control

- 3.2 – i 3.2. Points  $C_1$  and  $D_1$  represents the roots  $\lambda_3$  and  $\lambda_4$  of LPO i.e.
- $0.06 + i 0.47$  and  $-0.06 - i 0.47$ . The value of  $\xi$  is marked near the points  $A_1$ ,  $B_1$ ,  $C_1$  and  $D_1$  in Fig.8.7.

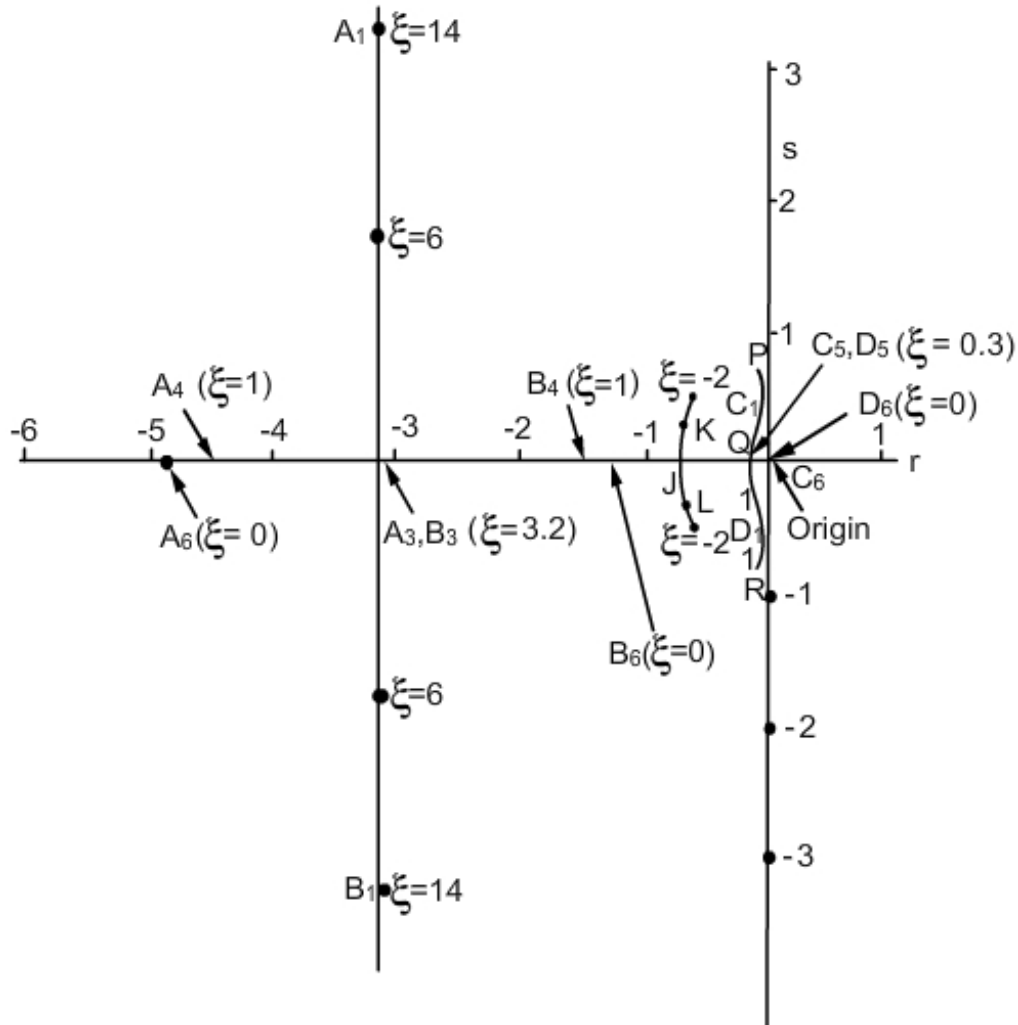


Fig. 8.7 Root locus plot –  $C_L = 1.0$  (Adapted from Ref.1.5, chapter 9 and inturn from Ref.8.1, with permission from controller of HM stationary office)

b) As  $\xi$  decreases the damping of SPO is not affected but the period increases. At  $\xi \approx 3.2$ , the SPO breaks into two subsidences. As the damping of SPO is not affected by  $\xi$ , the variation of the roots of the SPO for  $\xi > 3.2$  is indicated by a vertical line in Fig.8.7. For  $\xi < 3.2$  the roots are real and negative. Consequently, points corresponding to these values of  $\xi$  lie along the x-axis.

c) As regards the LPO, the damping slightly increases as  $\xi$  decreases. Further, the imaginary part ( $\omega_{LPO}$ ) slightly decreases as  $\xi$  decreases. At  $\xi \approx 0.3$  the LPO breaks into two subsidences. Thus, the curve representing the root locus plot for the LPO is not a straight line but a curve as shown by the line PQR.

d) As  $\xi$  decreases below 0.3, two real roots corresponding to LPO also lie on x-axis. When  $\xi$  equals zero, a zero root is seen.

e) When  $\xi$  is negative, there is a positive root corresponding to LPO. At  $\xi < -0.4$  the four roots are - one positive root, one complex pair and a large negative root. The damping of the oscillatory mode decreases with further decrease of  $\xi$ . This behavior is indicated by the curve KJL in Fig.8.7.

### 8.13.3. Two parameter stability diagram

While discussing the stability criteria, it was pointed out that for the characteristic equation to have stable roots, the coefficient 'E' in Eq.(8.9) and the Routh's discriminant 'R' in Eq.(8.26), should be positive. Thus, lines corresponding to  $E = 0$  and  $R = 0$  could be used to separate stable and unstable regions. The x- axis and the y- axis of such a diagram have two quantities which represent features of the airplane. This diagram is called two parameter stability diagram. Reference 1.5, chapter 9, suggest  $\xi$  and  $\nu$  as the two parameters. The quantity  $\xi$  is already defined in Eq.(8.64) and is proportional to  $C_{m\alpha}$ . The quantity  $\nu$  is proportional to  $S_t / S$  and is defined as:

$$\nu = \frac{1}{2} \frac{S_t}{S} \frac{C_{Lat}}{i_B} ; i_B = \frac{I_{yy}}{m l_t^2} \quad (8.65)$$

Figure 8.8 shows  $E = 0$  and  $R = 0$  lines on  $\xi$ - $\nu$  diagram for the LPO motion. As pointed out earlier, when  $E < 0$  a negative real root or divergence is predicted. Hence, a line corresponding to  $E = 0$  is referred to as divergence boundary. Further, when  $R = 0$ , the characteristic equation has either a zero root or an imaginary root with real part as zero. Hence, a line corresponding to  $R = 0$  is called Routhian boundary. Thus, a region of the two parameter stability diagram, where both 'R' and 'E' are positive is the region indicating dynamic stability. Figure 8.8 indicates the stable regions between the divergence boundary and Routhian boundary. It is further observed that for  $\xi > 0$ , it is not enough to have

Flight dynamics –II  
Stability and control

$E > 0$  but  $\nu$  must have an appropriate value to ensure dynamic stability.

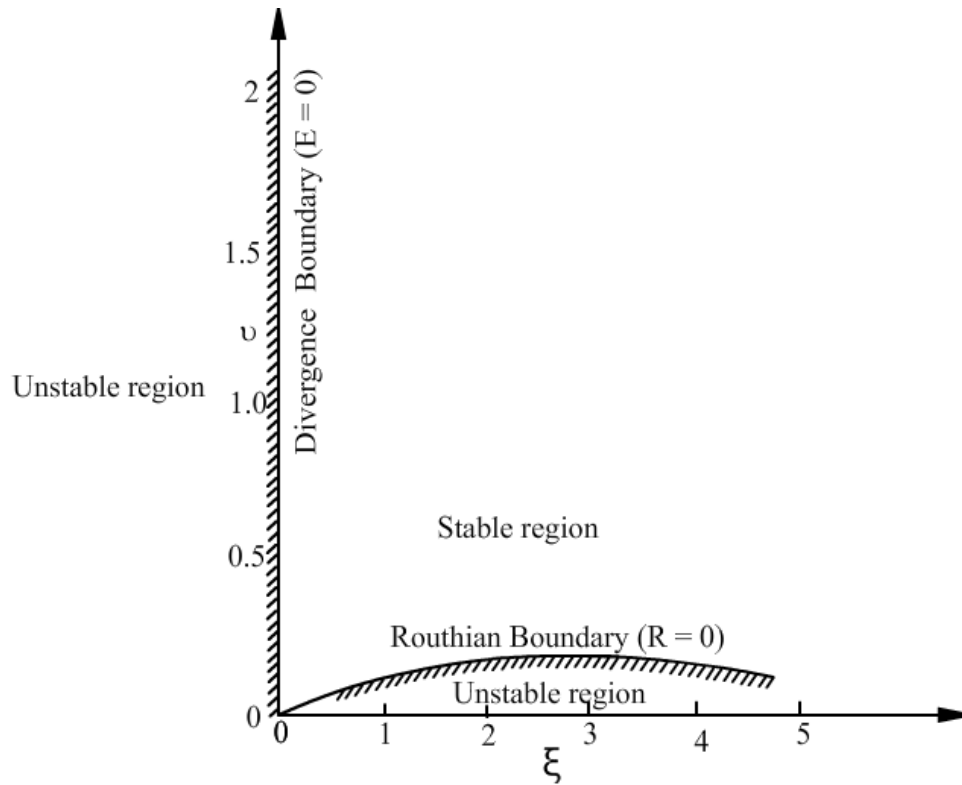


Fig.8.8 Two parameter stability diagram- LPO

(Adapted from Ref.1.5, chapter 9 and in turn from Ref.8.2, with permission from controller of HM stationary office)